ELEMENTA
Science of the Anthropocene

RESEARCH ARTICLE

Doomed to drown? Sediment dynamics in the human-controlled floodplains of the active Bengal Delta

Kimberly G. Rogers[*] and Irina Overeem[*]

The Ganges-Brahmaputra-Meghna (Bengal) Delta in Bangladesh has been described as a delta in peril of catastrophic coastal flooding because sediment deposition on delta plain surfaces is insufficient to offset rates of subsidence and sea level rise. Widespread armoring of the delta by coastal embankments meant to protect crops from flooding has limited natural floodplain deposition, and in the tidally dominated delta, dikes lead to rapid compaction and lowered land surface levels. This renders the deltaic floodplains susceptible to flooding by sea level rise and storm surges capable of breaching poorly maintained embankments. However, natural physical processes are spatially variable across the delta front and therefore the impact of dikes on sediment dispersal and morphology should reflect these variations. We present the first ever reported sedimentation rates from the densely populated and human-controlled floodplains of the central lower Bengal Delta. We combine direct sedimentation measurements and short-lived radionuclides to show that transport processes and lateral sedimentation are highly variable across the delta. Overall aggradation rates average 2.3 ± 9 cm y^{-1}, which is more than double the estimated average rate of local sea level rise; 83% of sampled sites contained sediment tagged with detectable ^{7}Be, indicating flood-pulse sourced sediments are widely delivered to the delta plain, including embanked areas. A numerical model is then used to demonstrate lateral accretion patterns arising from 50 years of sedimentation delivered through smaller order channels. Dominant modes of transport are reflected in the sediment routing and aggradation across the lower delta plain, though embankments are major controls on sediment dynamics throughout the delta. This challenges the assumption that the Bengal Delta is doomed to drown; rather it signifies that effective preparation for climate change requires consideration of how infrastructure and spatially variable physical dynamics influence sediment dispersal on seasonal and decadal time scales.

Introduction

The Ganges-Brahmaputra-Meghna (GBM), or Bengal, Delta in South Asia is a densely populated river delta formed from sediment deposited within the tectonically active Bengal Basin (**Figure 1**). Based on observations from river gauges on the main stem Ganges and Brahmaputra Rivers, a combined billion tons of sediment is annually transported from source areas in the Himalayas to the active delta in Bangladesh (Islam et al. 1999). River processes such as avulsion and overbank flooding naturally maintain the Bengal Delta's active floodplain, and reworking of fluvial sediment by tides onto the lower delta planform sustains the "abandoned" lobe of the mangrove-forested southwest delta (Rogers et al., 2013; Wilson and Goodbred, 2015). Collectively, fluvial and tidal processes have enabled overall delta

accretion to offset rising sea level since the mid-Holocene. Despite 1 Gt of sediment released to the delta each year, the modern Bengal Delta is labeled as a "delta in peril" of catastrophic coastal flooding because the volume of sediment transported to floodplains is insufficient to offset rates of subsidence and increasing coastal water levels (Syvitski et al., 2009). Tessler and others (2015) profile risk and socioeconomic vulnerability trends for 48 major deltas worldwide and find the >140 million people living on the GBM are increasingly at risk of coastal flooding related to local sea level rise and storm surges (Overeem and Syvitski, 2009).

Infrastructure designed to reduce the risk of devastating floods on the delta's surface also restricts sediment deposition on coastal floodplains. Beginning in the 1960's, government-built dikes were constructed around inhabited island perimeters of coastal Bangladesh in an effort to increase land area for rice paddy cultivation and to protect crops from tidal flooding (Rahman, 1994). To date, 139 embanked "polders" have been created in coastal Bangladesh, totaling ~6000 km of dikes

* Institute of Arctic and Alpine Research, University of Colorado, Boulder, Colorado, US

Corresponding author: Kimberly G. Rogers (kgrogers@colorado.edu)

encircling 1.12 million hectares of the delta (BWDB, 2013; **Figure 2**). Embankments have eliminated tidal flooding in many areas, but have also restricted the deposition of sediment that would naturally sustain the elevation of the landscape. This is particularly true in southwest Bangladesh, where eastward migration of the Ganges River has reduced connectivity of distributary river channel sources and sediment is delivered to the lower delta plain via a large network of tidal channels (Allison et al., 2003; Rogers et al., 2013; Passalacqua et al., 2013). These "headless" tidal channels contain saline or brackish water, and therefore dry season crop irrigation must depend on other relatively sediment-free water sources such as harvested rainwater or river water stored in on-farm canals (Mondal et al., 2008; Islam et al., 2010). Consequently, the interiors of many polders are starved of sediment that previously compensated for elevation loss related to compaction and tectonic subsidence. The elevation of this armored landscape is up to 150 cm lower than mean high water levels in adjacent channels, which makes arable land in the southwest delta susceptible to flooding if dikes are breached or overtopped by storm surges (Auerbach et al., 2015).

The central lower delta, by comparison, remains connected to distributaries of the main stem Meghna River and seasonally fluctuates between a mixed tidal- (winter) and fluvial- (summer) dominated system. River discharge is an order of magnitude less during the dry season compared to the summer (Coleman, 1969). During low-flow winter months, tides propagate 70 km upstream through secondary and tertiary channels of the lower main stem Meghna River and sediment is kept in suspension by spring-neap tidal fluctuations (Barua, 1990). Based on measurements of sediment discharge below the Ganges and Brahmaputra confluence and suspended sediment concentrations estimated within the active river mouth estuary, distributary channels of the main stem river are likely carrying up to an order of magnitude higher suspended sediment during the peak monsoon freshet compared with the dry season (Barua et al., 1994, Islam et al., 1999). Wet season river processes influence sediment transport in the central fluvial-tidal delta and should be reflected in sediment routing and flux across the delta plain, though polders control sediment dynamics here just as they do in tidal-dominated areas.
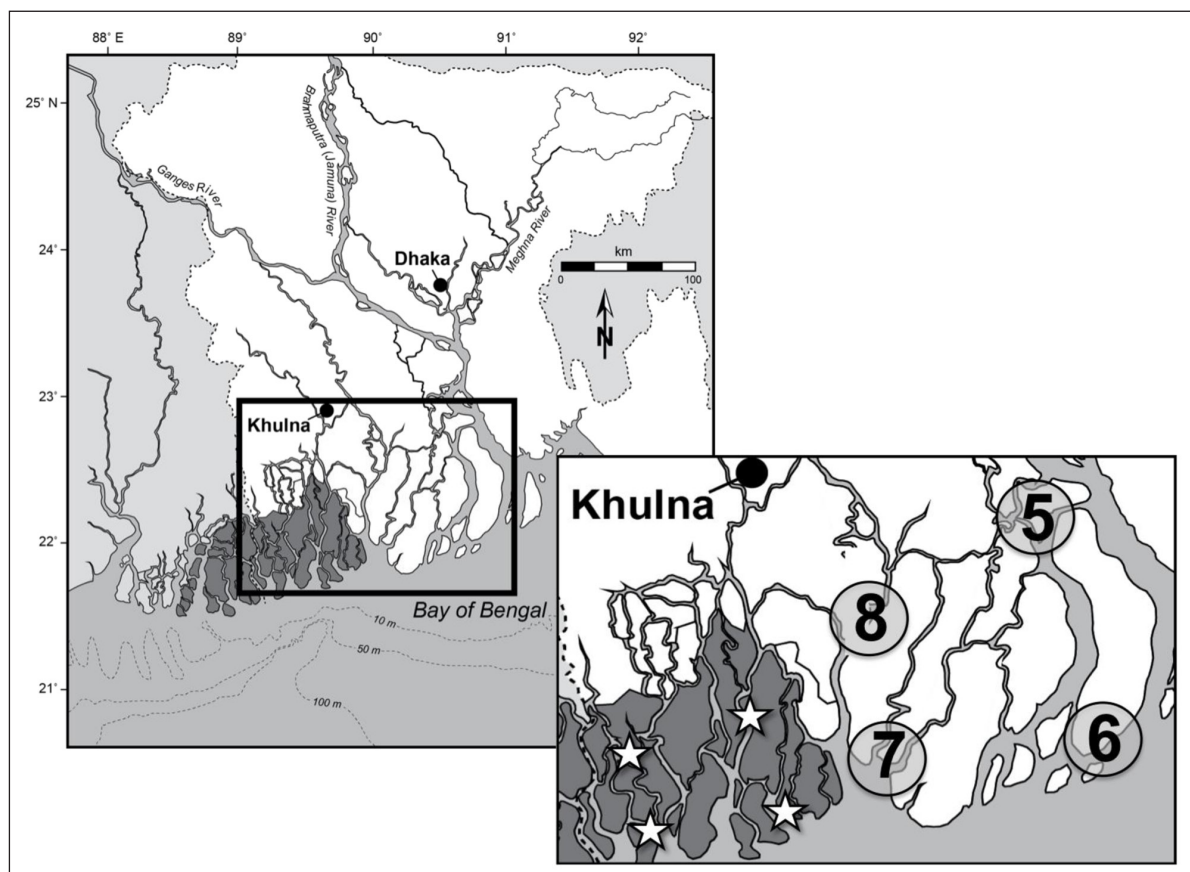

Figure 1: Study area in the lower Bengal Delta and coastal Bangladesh. White area is Bangladesh; light gray land areas are India, dark gray land area is the Sundarbans mangrove forest. Inset shows approximate locations of 2012 sediment trap deployment sites in the fluvial-tidal delta that are the focus of this study; numbers 5, 6, 7, and 8 mark the four sampling areas and correspond to the first digit in the individual site numbering scheme, e.g., 5.3.B; stars mark locations of 2008 sediment trap sites in the tidally-dominated delta (c.f., Rogers et al., 2013). Delta plain north of the Sundarbans and near to Khulna City is heavily embanked. DOI: https://doi.org/10.1525/elementa.250.f1
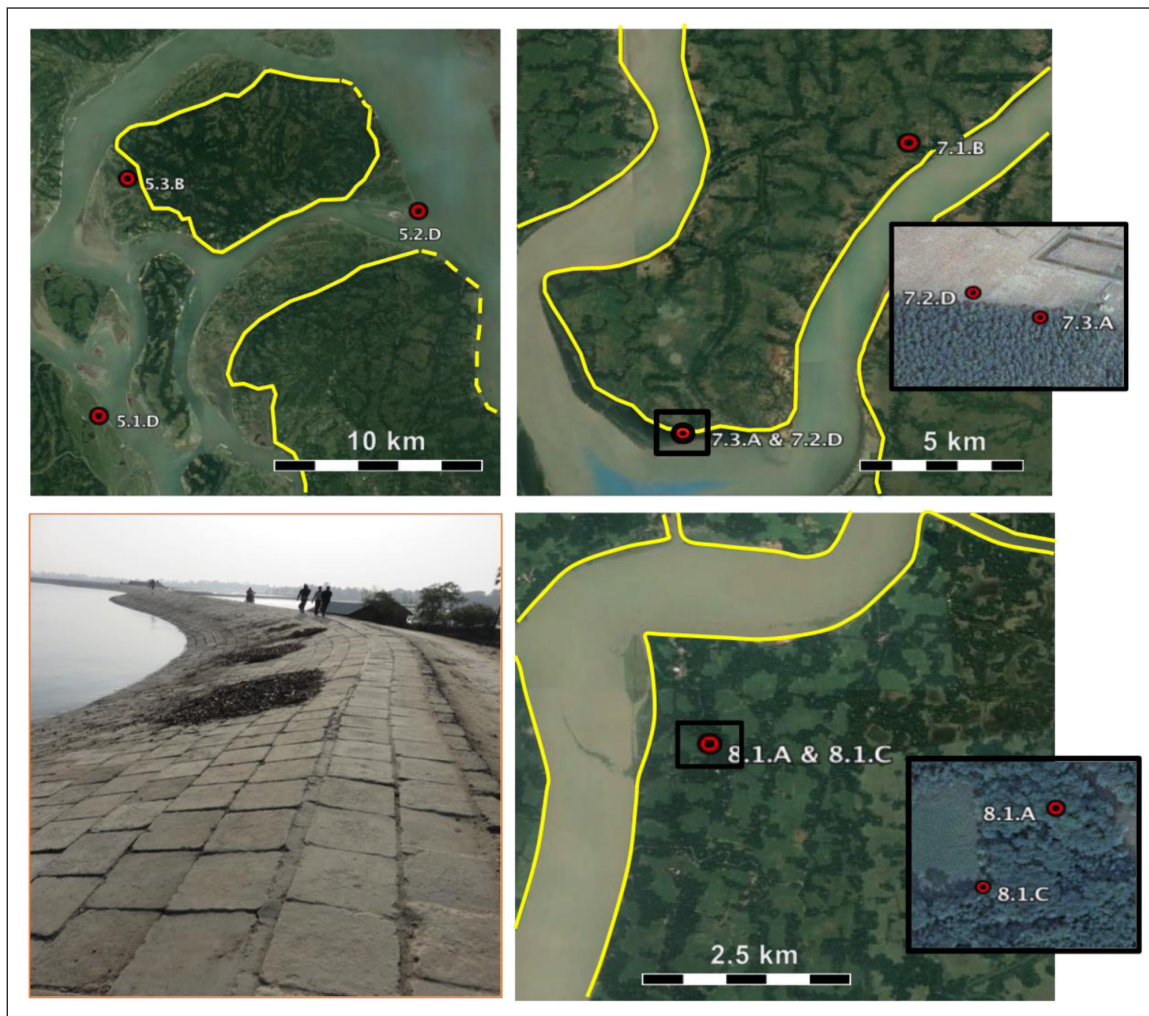
Rogers and Overeem: Doomed to drown? Sediment dynamics in the human-controlled floodplains of the active Bengal Delta

Art. 66, page 3 of 15

Figure 2: Locations of recovered sediment traps relative to embankments. Yellow lines mark position of embankments encircling polders; dashed line indicates missing embankment section as a result of river erosion. Bottom left corner is photo of typical embankment. First number of each trap site corresponds to the sampling area as described in Figure 1. DOI: https://doi.org/10.1525/elementa.250.f2

Until now, sedimentation patterns in the poldered fluvial-tidal region of the Bengal Delta have not been quantified, though this dynamic setting is one of the most densely populated (1500 people per km^2) and agriculturally diverse areas in coastal Bangladesh, and therefore considered one of the most vulnerable to coastal flooding (Poulton et al., 2010; BBS, 2011). Using direct sediment measurements and short-lived radionuclide geochronology, we map depositional trends of the 2012 monsoon floodpulse and fingerprint sediment sources on poldered islands of the mixed fluvial-tidal region of the Bengal Delta. We then present a simple approach to modeling sediment routing over delta distributaries and onto floodplains by using channel network characteristics to distinguish between three orders of channels and route suspended load according to their planview dimensions. We use an open source cross-sectional process model, AquaTellUs, to calculate cumulative cross-channel sediment flux deposited on delta islands over 50 years of river flooding. Our field results and model predictions of longitudinal sedimentation improve our understanding of floodplain accretion in the human-controlled fluvial-tidal region of the Bengal Delta, and challenges the assumption that it is doomed to drown.

Study site: Natural and engineered controls on sedimentation

Flooding on the Indian subcontinent is strongly influenced by the Asian monsoon, which brings heavy precipitation each year from June to October. The Ganges River, with headwaters in the northern Indian state of Uttarakhand, peaks from July to October. The Brahmaputra River originates in Tibet and is more pronouncedly affected by snowmelt from the Himalayas in May and June and subsequently by intense monsoon rains in the Eastern Himalayan Foothills. Widespread overbank flooding is an annually recurring event, especially in the active channel belts upstream of the confluence. Satellite mapping of flooding extent over a decade (1999–2009) shows a cumulative inundation area of ~50,000 km^2 by the combined rivers (Syvitski et al., 2009). Both river systems transport over 90% of their suspended sediment load during the

monsoonal period and have reduced river flow and therefore significantly lower sediment transport capacity during the dry season. The Meghna River, which originates in Bangladesh, contributes only ~1% to the overall annual sediment budget of the GBM system (Coleman, 1969). The combined GBM Rivers have built one of the world's largest deltas, with an area of approximately 110,000 km² (Kuehl et al., 2005). Just as in other large river systems, including the Mississippi and Amazon, physical processes such as overbank flooding, river migration, and avulsion have been shaping the Bengal Delta since the mid-Holocene and are inferred through stratigraphic and geochronologic evidence (Goodbred and Kuehl, 1999; Goodbred et al., 2003). The Bengal Delta is also among the largest of the Asian megadeltas experiencing heterogeneous subsidence (Woodroffe et al., 2006). Higgins and others (2014) mapped natural compaction in the most active depositional region of the GBM, near the confluence of the two main rivers. They found wide-ranging and spatially variable subsidence rates (0–1.8 cm yr⁻¹) controlled by fine scale differences in sediment grainsize and porosity, which reflect historical river processes. The active depositional environment and frequent channel switches have created a complex and spatially variable subsurface stratigraphy that influences surface topography, and hence, patterns of river avulsion (Kim et al., 2009). By contrast, subsidence rates along the perimeter of the Sundarbans in the tidal delta have been estimated at a 300-year average rate of 0.52 cm yr⁻¹, potentially reflecting both slow, natural compaction processes

combined with stochastic earthquake- or cyclone- induced subsidence events (Hanebuth et al., 2013).

Marine processes are additional first order controls on how water and suspended sediment are routed through the lower Bengal Delta plain. Tides in the Bay of Bengal, into which the Bengal Delta prograges, are semi-diurnal. The highest tides approach ~3 m amplitude in the region East of the active Meghna estuary mouth and decline in amplitude to ~1 m towards the Western part of the delta (Murty and Henry, 1983). The flood pulse of the three rivers significantly freshens the Meghna estuary and the surrounding mixed fluvial-tidal floodplains, and the system becomes river dominated during the 5 months of the monsoon. More distal from the Meghna estuary the relative impact of tidal dynamics increase, despite the lower tidal amplitude, and the direct influence of the river's freshwater flood pulse is less pronounced year round.

Sediment dynamics, and hence, morphological evolution of the lower delta, are influenced by this progression of natural processes across the delta front. Wilson and Goodbred (2015) differentiate the coastal zone into a lowland mixed fluvial-tidal delta and a downdrift tidal delta plain, reflecting the east-to-west transition (respectively) in river and tidal processes that dominate sediment distribution. Here, we focus on these two coastal regions, which are topographically characterized by a small slope (~10^{-5} m m⁻¹) and elevations below 5 meters above sea level, as mapped from the Shuttle Radar Topography Mission (**Figure 3**; Syvitski et al., 2009).
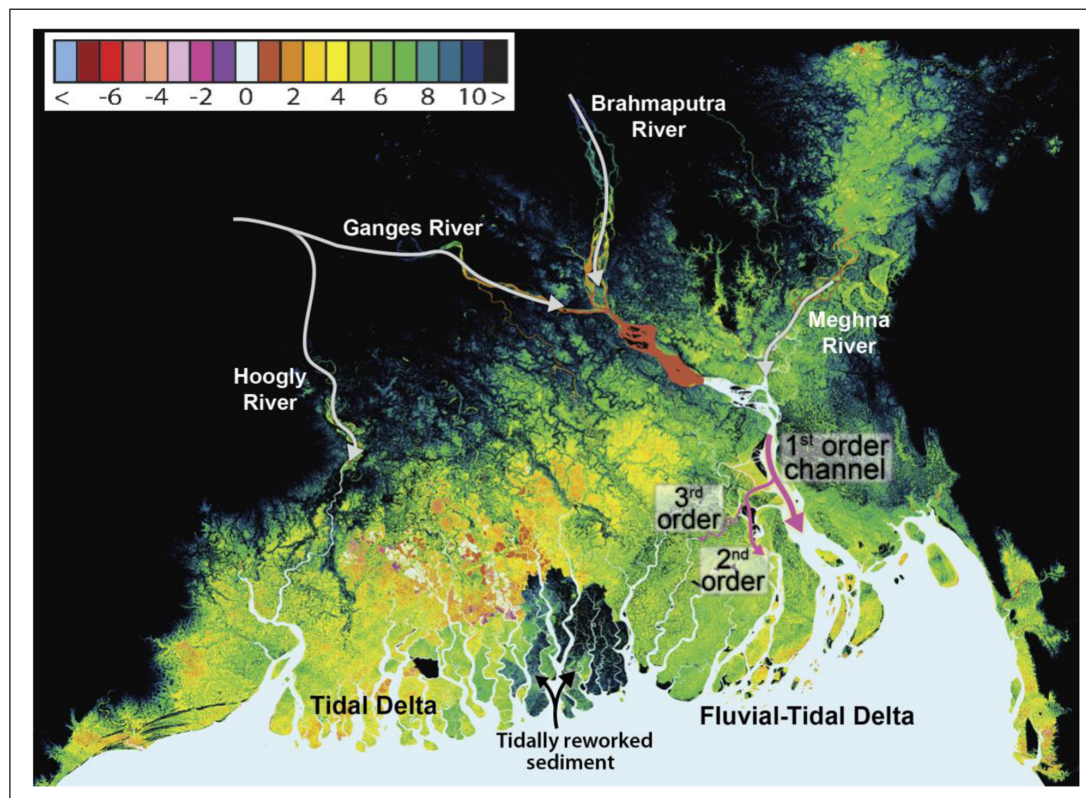

Figure 3: Topography of the Bengal Delta. 30-m Shuttle Radar Topography Mission (SRTM) altimetry data binned at 1 m vertical intervals, starting at sea level (light blue) to a height of 10 m, above which is black. Arrows indicate general input directions of sediment to the delta from main stem, distributary, and tidal channels (modified from Syvitski et al., 2009). DOI: https://doi.org/10.1525/elementa.250.f3

Rogers and Overeem: Doomed to drown? Sediment dynamics in the human-controlled floodplains of the active Bengal Delta

Art. 66, page 5 of 15

Distinct physiographic regions occur within these lower delta plains. The active fluvial dominated region of the Meghna Estuary contains a channel network comprised of a main stem and second- and third order distributary channels that have formed numerous channel bars and deltaic islands, whereas a dense, headless tributive channel network characterizes the downdrift tidal delta (**Figures 1** and **3**; Passalacqua et al., 2013). The tidal delta can be further subdivided into a cultivated region with embanked islands separated by numerous tidal channels, and the natural Sundarbans mangrove forests, a UNESCO World Heritage site. Beyond the Sundarbans, the lower Bengal Delta is heavily engineered to protect the food, water, and socioeconomic security of Bangladesh. The land outside the forest boundary is extensively clear-cut and cultivated, and houses almost 30% of Bangladesh's population in mostly rural farming communities (CGIAR, 2013). Widespread embankments were built with the intentions of increasing arable land for rice cultivation and protecting crops from tidal and storm surge flooding in the tide-dominated region of the delta, and for protecting land in the mixed fluvial-tidal zone from catastrophic river floods (Rahman, 1994). Sluice gates on embankments throughout both regions were designed to control river flooding cycles and local drainage of floodplains, and hence enabled sediment delivery to the delta plain. However, many sluice gates are clogged with sediment or no longer functional after years of poor oversight and insufficient maintenance (Ahmed, 2011).

Methods
Sediment sampling
Monsoonal sediment deposition on the embanked floodplain of the fluvial-tidal Bengal Delta was measured following a method used to record seasonal sedimentation in the mangrove forest of the unpoldered tidal delta plain (c.f., Rogers et al., 2013). In May 2012, prior to peak monsoon inundation, 52 sediment trap sites were installed along transects within four areas, or stations, bounding a region of ~3000 km^2: one inland and one coastal station directly west of the main stem Meghna River and estuary mouth (sites 5 and 6, respectively), and one inland and one coastal station directly east of the Sundarbans Forest Preserve (sites 8 and 7, respectively; **Figure 1**). Inland stations were located ~60 km and ~100 km from the coast. Individual trap sites consisted of a 30 cm long, 7 cm diameter PVC pipe buried with 1–5 cm exposed above the delta platform; a 10 cm × 10 cm piece of artificial turf secured to the delta platform with 10 cm steel pins, and a 10 cm × 10 cm ceramic tile also secured to the platform with steel pins (**Figure 4**). The three types of traps were used to provide redundancy in sampling in case one or more method failed. Traps were in place for the entire 2012 monsoon flood season (May–October) and there were no major coastal storms during this time.

Stations adjacent to the Sundarbans are influenced mainly by tides in the dry season, though there is connectivity to second and third order distributaries of the main stem river. Stations near to the Meghna River are
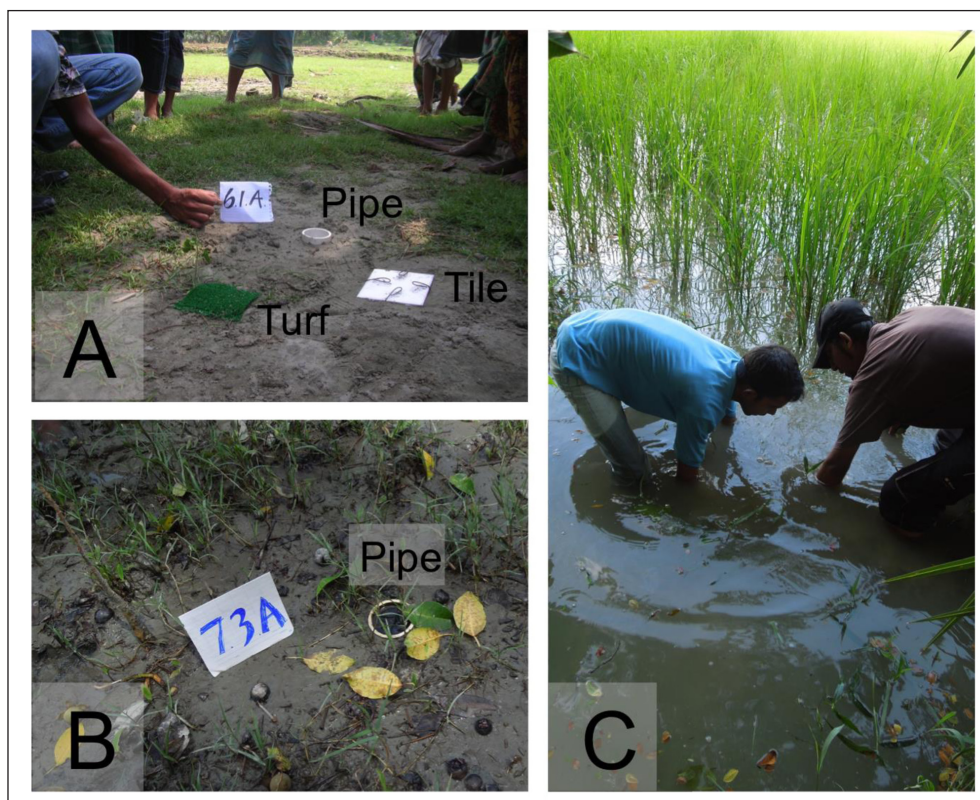

Figure 4: Examples of sediment sampling sites. A) Typical sediment trap array including turf, tile and pvc pipe secured to the floodplain surface prior to monsoon flooding. **B)** Example of a recoverable post-monsoon trap site with visible rim of pvc pipe, and **C)** An unrecoverable post-monsoon trap site still inundated with floodwater. DOI: https://doi.org/10.1525/elementa.250.f4

influenced by both tides and river discharge during the dry season and become exclusively fluvial during the summer flood pulse. We assume that any sediment deposited on the lower floodplain via dry-season tides in the months prior to installation of our traps was minor and overwhelmed by monsoon sedimentation. Monsoon flooding of the central lower delta plain began in June 2012, and many sites were still inundated during trap retrieval in October 2012. At two sites where monsoon floodwaters had drained but traps were missing, a 10 cm trench was dug to estimate the thickness of new sediment overlying the pre-monsoon soil layer (**Figure 5**). Relative thickness of seasonal deposits observed in trenches was corroborated with local farmers' estimations of new sediment layer depths. Sediment traps and trench measurements recorded net seasonal average deposition, integrating seasonal variations arising from flood and inundation duration, and fluctuating suspended sediment concentrations. Additionally, a 10 cm × 10 cm × 1 cm surface sample was collected in October 2012 at all accessible trap sites for radionuclide analyses.

Individual trap sites were chosen to capture sedimentation across a representative range of land use and flood control settings typical of the region. These included rice paddies, banana and mahogany tree plantations, fallow and/or heavily grazed fields, and irrigation ditches. An isolated mangrove stand was also sampled within the coastal study area near the Sundarbans. Traps were placed in rough transects that followed one of two patterns: (1) extending up to 15 km, aligned sub-parallel to natural channel banks and artificial embankments built by villagers for water diversion, flood control and transportation, with trap sites spaced along transects at ~2–5 km intervals, or (2) extending ≤500 m in length, perpendicular to natural channels, with trap sites spaced ~50 m apart. In many places, a mirrored sampling array was used where two sediment traps were installed near to each other, with one adjacent to a small order natural channel and a second separated from the first by a low (<2 m) mud dike. This sampling approach was designed to provide comparison between sedimentation on managed land plots from natural channel overbank flooding and that from irrigation canals.

Beryllium-7 geochemistry

Beryllium-7 is a naturally occurring cosmogenic fallout nuclide ($t_{1/2}$ = 53.3 days; 477.7 KeV) that can be used for identifying recently eroded (i.e., ≤6 months) sediments transported downstream from their catchment areas. It has been used to measure flood deposits on the inner shelf (e.g., Sommerfield et al., 1999), soil redistribution following catchment erosion (e.g., Schuller et al., 2006), and to track monsoon-derived sediment deposition on the abandoned Bengal tidal delta plain (e.g., Rogers et al., 2013). We set 0.2 dpm g^{-1} as the limit for detectable ^{7}Be to account for minor atmospheric contributions directly to the fluvial-tidal delta plain. Walling (2013) and references therein provides additional details regarding the use of ^{7}Be for tracking short-term sediment transport phenomena. Here, we use ^{7}Be to determine the relative contribution of flood pulse sediments deposited on the lower fluvial-tidal delta plain during seasonal flooding of the rivers and canals. Sediments deposited within recovered traps, and sediments collected from the top 1 cm of soil at all accessible sites were homogenized and dried at 60°C and analyzed at Vanderbilt University for ~24 hours on an Ortec 125-mm^2 planar germanium gamma detector. The detector was calibrated using a custom mixed gamma source and IAEA-375 soil standard. Between 50–150 g of dried ground sediment per sample was analyzed within three weeks of collection to minimize decay of active ^{7}Be.

Numerical model

A numerical model, AquaTellUs, is used to model lateral sedimentation patterns that result from cross channel overbank flooding. AquaTellUs is a floodplain deposition model that routes a channel belt through a landscape with a steepest-descent algorithm. Using an Exner approximation, AquaTellUs estimates net erosion and sedimentation as a function of river discharge, sediment load, and local bedslope (Overeem et al., 2003, 2005). The model simplifies depositional processes specifically for lowland fluvial-deltaic environments, and is designed for relatively large spatial and temporal scales: 10s to 100s of kilometers over

Figure 5: Example of sediment trench. Orange line denotes pre-monsoon layer with mottled contact overlain by sediment deposited during 2012 monsoon. DOI: https://doi.org/10.1525/elementa.250.f5

Rogers and Overeem: Doomed to drown? Sediment dynamics in the human-controlled floodplains of the active Bengal Delta

Art. 66, page 7 of 15

10s to 1000s of years. We simplify delta system dynamics by assuming that over long timescales flood periods are the dominant depositional mechanism. The model is designed to mimic sediment transport and depositional processes throughout a generic lowland river channel belt domain and into the shallow marine domain, similar to the lower Bengal Delta and other coastal deltaic settings. For the purpose of this paper, the model is set up to: 1) provide insight regarding downstream trends in aggradational thickness, and 2) map lateral sediment distribution throughout the smaller distributary delta channels. Coupled with sedimentation data collected at our field sites, this process-response model can improve our understanding of surface processes that dynamically respond to internal and external forcings. Detailed descriptions of the model approach, main equations and simulation input parameters are presented in the Supplementary Material and Tables S1 and S2.

Experimental setup

For these highly simplified experiments we run AquaTellUs with a theoretical grid over 50 years. The initial grid comprises 60 by 90 km, and initial slopes of 0.05 m km^{-1} in the fluvial domain and 0.15 m km^{-1} in the marine domain. Slope is set from topographic profile extraction from Shuttle Radar Topography Mission data and is representative for the fluvial-dominated sector of the GBM system (Syvitski et al., 2009; Wilson and Goodbred, 2015). Random topographic noise with a maximum level equivalent to the slope elevation is applied across the initial grid. The upstream boundary condition defines the location where the river enters the grid. This location remains stable over a number of time steps, depending on the magnitude of the flood year. In large flood years a new channel pathway is calculated based on a steepest descent algorithm. The simulations are run for 3 grainsize classes: sand, silt and clay. Partitioning of sediment grainsize classes is inferred from sparse direct measurements of suspended load in the main stem river, and preserved Holocene stratigraphy of the lower delta plain (Goodbred and Kuehl, 1999; Khan and Islam, 2008). We take into account the larger proportion of clays and silt within suspended sediment concentration measurements, but note the relatively high proportion of silt and very fine sand within the deltaic setting. We use these data to partition the grainsize classes within our simulated river flows as 30% sand, 20% silt, and 50% clay.

Table S2 lists the detailed experimental setup, common to both scale experiments. We assumed average river discharges of 1500 m^3 sec^{-1} in large scale channels, and 500 m^3 sec^{-1} in our smaller-scale experiments. These selected values are approximate, as there are a variety of channel widths within the delta plain's distributary network. Similarly, the suspended sediment concentration (SSC) is within the magnitude of observed values (i.e., Coleman, 1969; Barua, 1990). Measurements of SSC are generally collected far upstream from the distributary channels near the Farakka Barrage just upstream of the Indo-Bangladesh border, or nearby the confluence of the three rivers; the specified discharge and concentration values are scaled up to 2 orders of magnitude for the smaller distributary channels in these experiments.

Our basic set of simulations aims to quantify sedimentation trends for different scales of natural distributary channels within the deltaic network. The AquaTellUs model and its resolution do not allow for direct assessment of the effect of human engineering. To simulate the effect of embankments and sluice gates on overbank flooding and resultant sediment deposition, one would need to manually manipulate the grid to built topographic barriers and gates along the channel belts. However, this is inappropriate at the resolution of the model (i.e., 500 m by 500 m). Instead, we pose a thought experiment in which a natural distributary network is compared to a human-engineered network by redefining the magnitude of the flood discharge at which floodplain inundation can occur. In doing so, the model mimics the effect of embankments prohibiting overbank floods.

Results

Field results

Eight (i.e., 15% of the total deployed) sediment traps were retrieved in October 2012 following cessation of monsoon floodwaters (**Figure 6**). Sediment traps were retrieved from a variety of land use settings both within and outside of polders, which suggests land use type and embankments are not primary controls on deposition in this part of the delta (**Table 1**). Missing traps were likely destroyed during cropland plowing, removed by curious villagers, lost during flood erosion, or were still inundated by monsoonal floodwaters during the recovery effort (e.g., **Figure 4c**).

Recoverable trap sites received a cumulative average of 2.9 ± 2.4 g cm^{-2} of new sediment during the flood pulse, which converts to a vertical accretion rate of 2.3 cm y^{-1} when divided by the dry bulk density of 1.3 g cm^{-3} assumed for GBM River sediments (per Allison and Kepple, 2001). Three discernable trends emerge from our trap results. First, sites adjacent to small, natural second or third order channels received more new sediment (mean: 3.6 ± 2.4 cm) during the 2012 monsoon season compared to trap sites receiving sediment via controlled irrigation canals (mean: 1.4 ± 1.9 cm), though both received floodpulse-sourced sediment (see description of gamma spectroscopy results, below). Second, sites in fallow fields outside of polders accumulated more new sediment than cultivated sites located inside polders, demonstrating that sediment accumulation across the delta plain would likely be much higher here under natural conditions. Third, traps located <10 m from their nearest channel accumulated slightly more sediment (mean: 2.6 ± 2.8 cm) than sites located >100 m from their nearest channel (mean: 2.1 ± 1.2 cm), as would be the expected pattern from overbank flooding. Additionally, accumulation measured at trench sites averaged 5.5 cm, corroborating local farmers' estimations of new sediment thicknesses; however, these were not included in our calculations due to the high uncertainty associated with these values.

Gamma spectroscopy reveals that 75% of new sediment recovered in the delta plain traps was tagged with ^{7}Be

Table 1: Summary of results from recovered traps and trench sites. DOI: https://doi.org/10.1525/elementa.250.t1

Site (* = trench site)	Land use	Inside/outside polder	Distance from nearest channel (m)	Channel type and order	Sediment vertical accretion (cm)	Be-7 activity (mean, dpm/g)
5.1.A*	Fallow, for grazing	Outside	10	Natural; 3rd	6	0.63 ± 0.24
5.1.D	Fallow, for grazing	Outside	2	Natural; 3rd	6	Below detection
5.2.D	Rice paddy	Outside	100	Natural; 2nd	1	Below detection
5.3.B	Rice paddy	Outside	300	Natural; 3rd	1.2	0.76 ± 0.34
6.1.A*	Rice paddy	Outside	60	Natural; 3rd	5.1	1.36 ± 0.57
7.1.B	Rice paddy	Inside	8	Irrigation canal	0.2	0.90 ± 0.5
7.2.D	Rice paddy	Outside	500	Natural; 3rd	2.3	1.24 ± 0.33
7.3.A	Mangrove stand	Outside	500	Natural; 3rd	3.7	0.58 ± 0.28
8.1.A	Mahogany plantation	Inside	5	Irrigation canal	3.7	0.25 ± 0.24
8.1.C	Rice paddy	Inside	1	Irrigation canal	0.4	0.42 ± 0.19

above the detection limit of 0.2 dpm g^{-1}, including sediment delivered via irrigation canals (**Table 1**). Additionally, 83% of sites where sediment was collected from the surface of the delta, but where traps were missing, contained detectable ^{7}Be (Table S3). Activities of ^{7}Be measured on all samples range from below detection to 2.64 dpm g^{-1}, with a mean activity of 1.04 ± 58 dpm g^{-1}. Assuming the ^{7}Be inventory was spatially uniform across the delta plain prior to the onset of monsoon flooding (e.g., Walling, 2013), these variations likely reflect the mixing of recently eroded catchment-sourced sediment with differing fractions of older (>6 months) ^{7}Be-deficient sediment sourced from river channel banks or locally re-worked. In cultivated settings, lower ^{7}Be activities suggest dilution with older sediment potentially brought to the surface through deep tilling of cropland. Though there are no measurements of fallout activities published for Bangladesh, we assume ^{7}Be on newly deposited sediment was sourced from adsorption to sediment particles in the catchment, rather than *in situ* fallout: ^{7}Be activities on central lower delta plain sediments are comparable to activities measured on both suspended samples collected in the main stem river during peak flooding (i.e., mean 0.7 ± 0.3 dpm g^{-1}; max 1.4 dpm g^{-1}) and on sediment deposited within the mangrove forests and tidal channel banks within the tidal delta plain during the 2008 monsoon (e.g., mean 0.7 ± 0.4 dpm g^{-1}, max 1.9 dpm g^{-1}; c.f., Rogers et al., 2013). Combined with increasing our ^{7}Be detection limit on sediments to 0.2 dpm g^{-1} to account for additional fallout contributions, these results collectively highlight the efficiency of the GBM dispersal system in routing catchment-sourced sediment to remote areas of the delta system.

To summarize these field results: mean vertical sedimentation in recovered traps is 2.3 cm, and approximately three-quarters of all delta plain sediments recovered from traps and surface samples contained detectable ^{7}Be. Taken together, our results point to a floodpulse source for sediments routed onto poldered floodplains, and reflect the importance of overbank flooding of second and third order distributaries and irrigation canals in maintaining the central lower delta plain. Although recovery was limited to 15% of the total number of traps deployed, these are the first direct sedimentation observations for this densely populated and heavily cultivated region of the delta, and provide a baseline for more widespread sedimentation studies here. Furthermore, when considered alongside monsoon sedimentation measured on the uncultivated Sundarbans mangrove platform (i.e., 1.0 ± 0.9 cm yr^{-1}; c.f., Rogers et al., 2013) and sediment starvation inside the poldered islands that lie outside the boundaries of the Sundarbans within the tidal delta (c.f., Auerbach et al., 2015), our results show that the processes governing sedimentation on the Bengal Delta as a whole are spatially variable, and sedimentation patterns reflect this heterogeneity.

Model results
Here, we augment our seasonal sedimentation results with simple model experiments to explore the lateral sedimentation patterns that would result from natural overbank flooding and avulsion of channels in the central lower Bengal Delta over a 50-year time period. We use channel network characteristics based on an analysis of satellite imagery by Passalacqua and others (2013) to distinguish between two orders of channel widths, and route suspended load according to their planview dimensions. Edge-to-edge channel widths were visually assessed and grouped into one of four orders of magnitude ranging from meters within islands, to several kilometers in the main channels. We designed two experiments using binned channel widths to estimate cross-channel sediment flux deposited on delta islands during flooding of second and third order river channels, as defined using the Hack (1957) classification scheme for stream order. Since AquaTellUs models a single channel belt, we employ a simple approach to explore sediment routing over multiple delta distributaries and into tidal channels. Model theory and variables used in the experiments are described in

Rogers and Overeem: Doomed to drown? Sediment dynamics in the human-controlled floodplains of the active Bengal Delta

Art. 66, page 9 of 15

Table S1 and in the supplemental section accompanying this article.

Model experiments

In experiment one, the location of the main channel belt shifted six times during larger flood years, and the sedimentation across the respective pathways and in the nearshore zone is evident (**Figure 7A**). One central channel belt persisted over the longest period and was re-occupied in the later stages of the simulation. **Figure 7A** shows that 50-year planview cumulative deposition adjacent to these second order channels can be as high as 150 cm in the most stable channel belt, a rate equivalent to ~3 cm yr^{-1}. Significant amounts of sediment are deposited over floodplains with widths as large as 2500 m, which demonstrates the efficiency of smaller order distributive channels to laterally disperse sediment across the delta plain. Cumulative sedimentation tapers off with downstream distance in the fluvial domain, and much less sediment is deposited in the fluvial-deltaic plain close to the coast as compared to the axial zone near the apex. Deposition in the nearshore zone, by mouthbars and delta plumes, is much higher again and amount to 80 to 140 cm (i.e., 1.6 to 2.8 cm yr^{-1}) in the most active river mouth region. Annual accretion rates over the 50 years of our model experiments are similar to those recorded in our sediment traps near both natural channels (i.e., 1 to 6 cm yr^{-1}) and irrigation canals (i.e., 0.2 to 1.7 cm yr^{-1}) during the 2012 monsoon season.

Stratigraphic sections are shown in **Figure 7B** at 5 km, 20 km and 45 km downstream from the delta's apex. A strong downstream fining trend can be distinguished; deposits near the delta apex are distinctly sandy, whereas the deposits in the coastal plain range from very fine sand to fine silt. The cross-sectional stratigraphy produced by AquaTellUs contains repeated sequences of upward-fining

medium to fine sand, and increasing concentrations of fine sand and silt deposited laterally with distance from channel levees. These results are similar to sequences identified in sediment cores retrieved from the active delta plain (c.f. Allison et al., 2013). Experimental stratigraphic sections near to the delta's apex (i.e., 5 km and 20 km) reflect deltaic construction facies with higher sand content, whereas the most downstream stratigraphic section is characteristic of distributary channel infill and overbank flooding, or maintenance facies, as described by Wilson and Goodbred (2015). The stratigraphic sections show that when these first-order channel belts shift regularly due to peak flooding events, sandy deposits amalgamate pronouncedly in the upstream floodplain. Amalgamation does not occur in the most downstream fluvial-delta plain. The channel belts are widely spaced and form more isolated super-elevated depositional bodies.

The depositional pattern over 50 years of simulation for the third order channels shows deposits are much less thick (**Figure 8**). The simulated grid represents a similar domain of 90 by 60 km from the fluvial-deltaic plain upstream into the shallow marine domain. In this scenario the channel belts appear more stable, despite a similar flooding regime; only two major belts prevail over the entire simulation. This is typical in simulations with less sediment deposition, because previously deposited sedimentary bodies will not perturb re-calculation of the flow path. For the third order channel experiments, the model predicts that lateral deposits still spread over 1500 m or more in large flood years. These experimental results are most salient to our observed sedimentation data, as new sediment deposition in 2012 was recorded up to 500 m away from the nearest third order channel, i.e., the upper limit of trap deployment relative to the nearest channel. This reinforces the assumption that smaller-order streams have the potential to widely disperse sediment across the
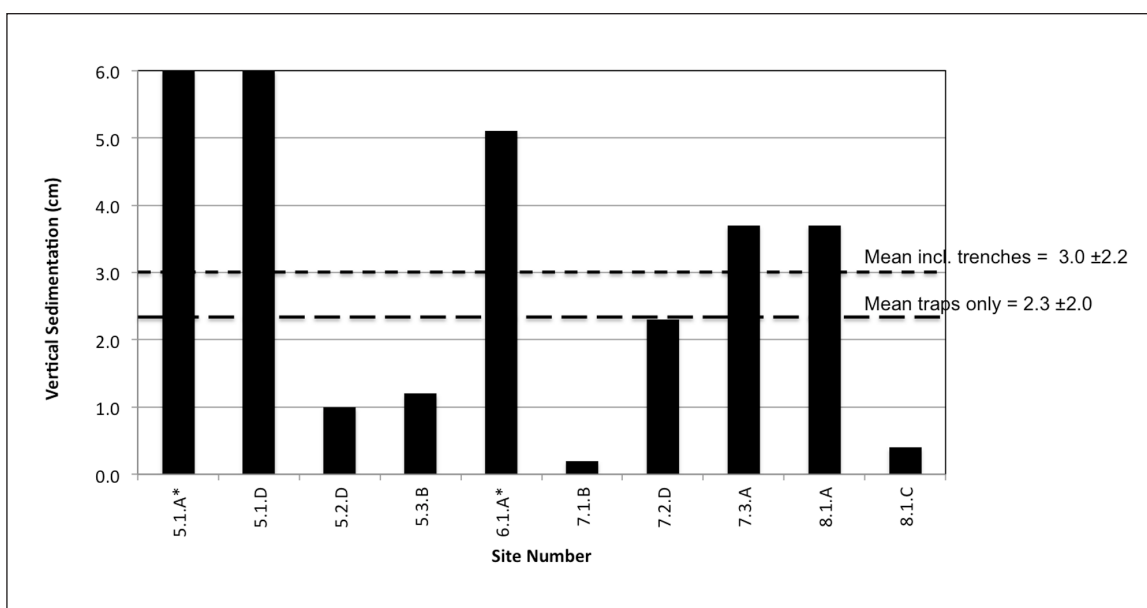

Figure 6: Vertical sediment accumulation for recovered tiles and trench sites (*). Mean cumulative accretion value is noted for recovered sediment traps and trenches, and for traps only. DOI: https://doi.org/10.1525/elementa.250.f6
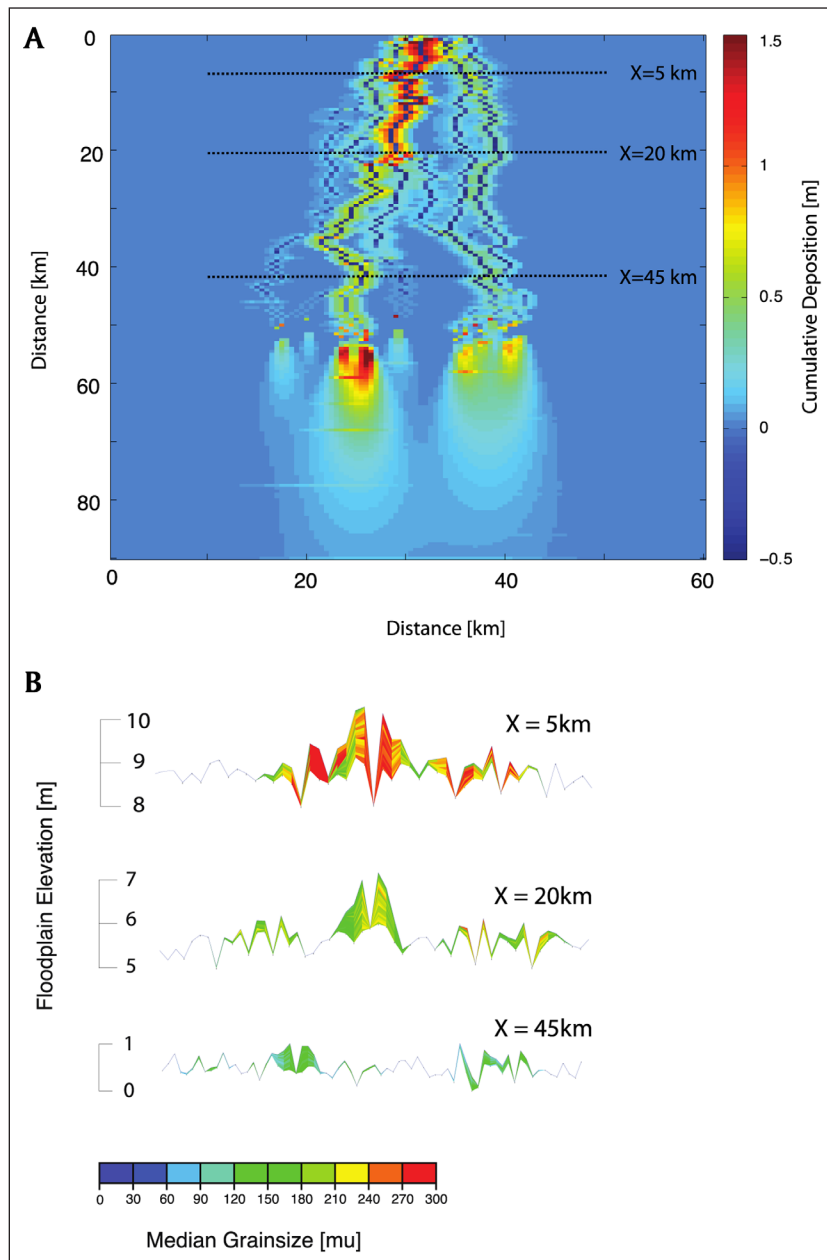
Figure 7: AquaTellUs results from experiment 1. A) Plan view map of the pattern of cumulative deposited sediment over 50 years of simulation for a channel belt representative of the second order channels. The simulated grid represents a zone of 90 by 60 km from its apex into the shallow marine domain. **B)** Simulated stratigraphic cross-sections. DOI: https://doi.org/10.1525/elementa.250.f7

floodplains when the system becomes river-dominated during the monsoon floods.

We implemented an additional set of paired simulations (experiment 3) to further scrutinize the effects of human engineering on floodplain sedimentation. These simulations build upon experiment 1, which is representative for a second-order channel belt. In this case however, we contrast the base case simulation where floodplain inundation occurs every monsoonal season, i.e., the perceived natural regime, with a simulation in which overbanking and lateral sedimentation is restricted to a narrow channel belt with much higher seasonal flood discharge. **Figure 9** summarizes the respective cumulative sedimentation maps (Movies 1 and 2 documenting

these simulations are located in the Supplementary Material). The comparison emphasizes the diffuse nature of lateral sedimentation in the natural inundation regime (**Figure 9A**), whereas in the "embanked" simulation, sediment aggradation only occurs directly adjacent to the channel belt. This is a logical consequence of how the model run is set up, but it emphasizes the observed mechanism of within-channel belt infilling due to the embankments (e.g., Hale et al., 2015). Another important consequence of restricting flood inundation is the increased deposition within the marine domain, as sediment more efficiently travels further downstream in a constrained channel belt. It is obvious from **Figure 9B** that a more extensive mouthbar complex and shallow marine deltaic
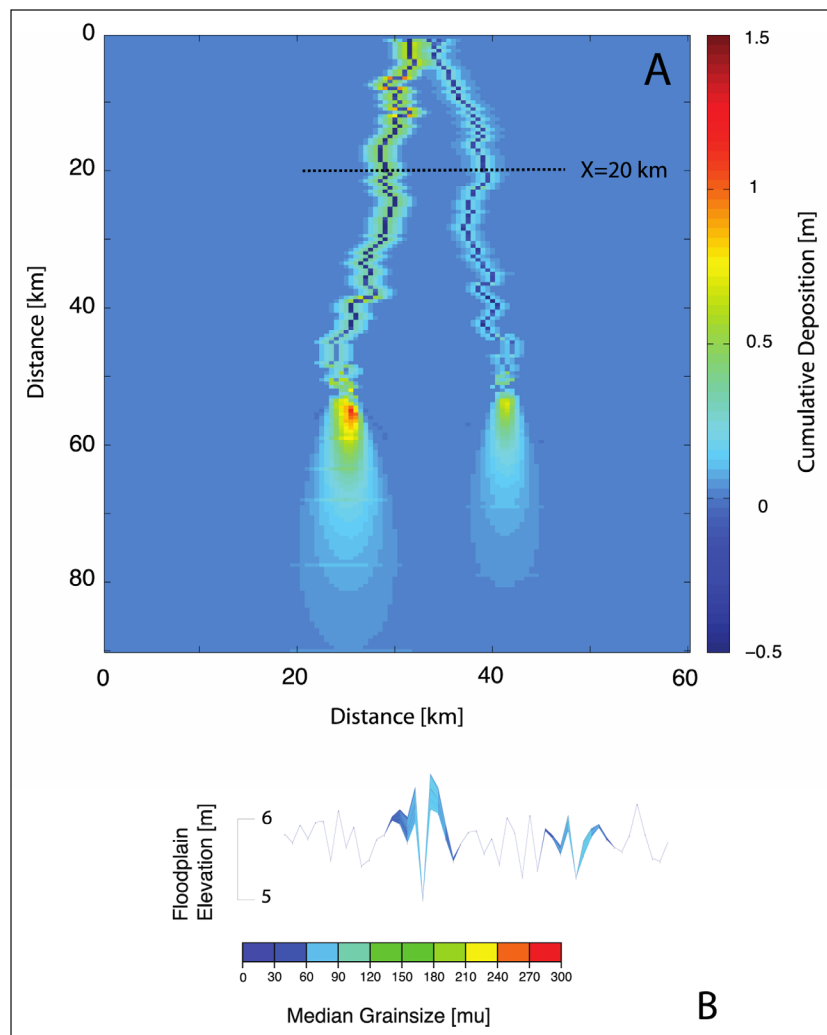
Rogers and Overeem: Doomed to drown? Sediment dynamics in the human-controlled floodplains of the active Bengal Delta

Art. 66, page 11 of 15

Figure 8: AquaTellUs results from experiment 2. A) Planview map of the pattern of cumulative deposited sediment over 50 years of simulation for a channel belt representative of third order channels. The simulated grid represents a zone of 90 by 60 km from its apex in the fluvial-deltaic into the shallow marine domain. **B)** Simulated stratigraphic cross-sections. DOI: https://doi.org/10.1525/elementa.250.f8

wedge is built over the duration of the simulation. Lastly, these contrasting simulations show how natural channel switching is potentially subdued by embankments; within the model this is because of less pronounced sedimentation in the apex of the channel belt, allowing the channel belt to retrace its original position, even when a possible switch is triggered due to a high flood year occurrence. This behavior induces yet another supply mechanism for lateral sediment dispersal to maintain a stable deltaic floodplain and is restricted in the "embanked" scenario. Interestingly, small channel switches near the rivermouth are more prominent in **Figure 9B**, due to more rapid emergence of the mouthbar complex.

Discussion
Tidal delta vs. mixed fluvial-tidal delta
These model simulations and observed seasonal sedimentation patterns are the first to be produced for the poldered fluvial-tidal region of the central lower Bengal Delta. Our results show that new sediment is delivered to this area of the delta plain during the monsoon flood

through overbank flooding of second and third order natural channels, as well as through irrigation canals that provide rice paddy fields with fresh river water; proximity to the main stem river enables farmers to take advantage of increased freshening of channel waters during high discharge. In other words, embankments do not entirely restrict vertical accretion and lateral sediment dispersal on poldered islands in the fluvial-tidal delta such as they do in the embanked areas of the southwest tidal delta. As demonstrated by Auerbach and others (2015), embankments limit sediment deposition on inhabited poldered islands in the tidal delta and as a result, interiors of polders are as much as 150 cm lower in elevation than mean high water levels in adjacent tidal channels. Most of the suspended sediment that is imported landward on flood tides is instead deposited within channels, resulting in the infilling and closure of >600 km of intertidal channels and emergence of ~90 km^2 of new land in the southwest delta (C. Wilson, 2017). Though the embankments have protected farmland from saline flooding, lowered land surfaces now render inhabited tidal islands
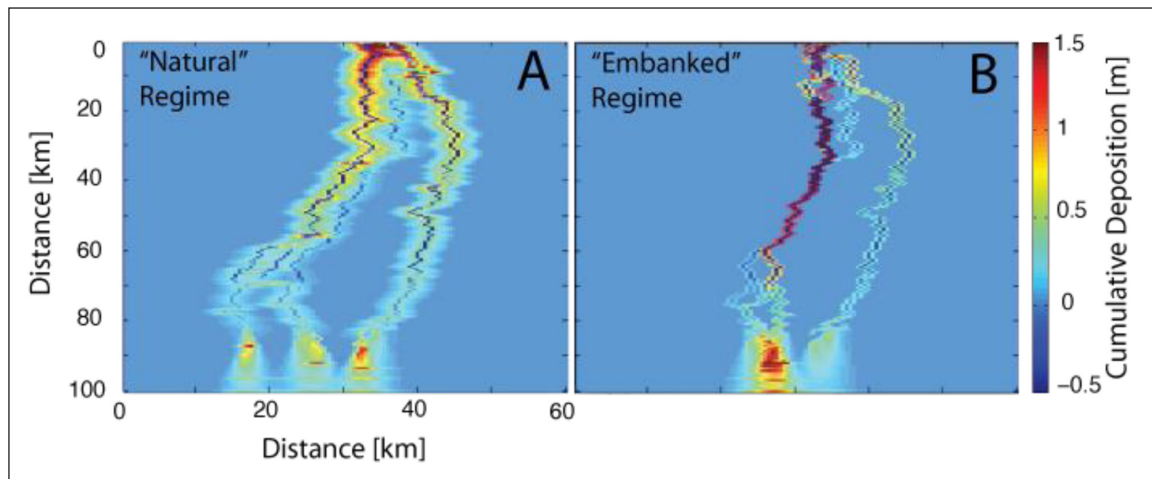
Figure 9: AquaTellUs results from experiment 3. A) Planview map of cumulative sediment deposition patterns over 50 years of simulation for a channel belt representative of a natural floodplain inundation regime. Diffuse spreading of the flood sediment occurs, and more channel belts form. **B)** Planview map of cumulative sediment deposition patterns over 50 years of simulation for a channel belt representative of a restricted inundation regime, showing less fluvio-deltaic plain sedimentation, some within channel belt sedimentation and more pronounced mouthbar and marine sedimentation. Channel switches are reduced in this regime. DOI: https://doi.org/10.1525/elementa.250.f9

water logged and vulnerable to flooding by storm surges. This contrasts with the spatially averaged 1.1 cm per year of new sediment maintaining the surface elevation of ~4800 km^2 of forested intertidal delta plain in the unembanked Sundarbans mangroves, immediately adjacent to cultivated poldered areas (c.f., Rogers et al., 2013). If we take the results of the current study as representative of mean annual sedimentation in the central fluvial-tidal delta, the cumulative vertical accretion rate (2.3 cm y^{-1}) is over two times higher than sedimentation within the natural intertidal setting of the Sundarbans. Based on the proximity of our study sites to the main stem river system, higher accumulation rates are expected compared to the "abandoned" lobe of the tidal delta, which has not been connected to Ganges river distributaries for several hundred years.

Interannual variability in monsoon discharge

Fluctuations in river discharge can impact net sediment accretion from year to year. To determine whether accumulation recorded in 2012 is representative of longer-term mean annual sedimentation, we investigated a time series of discharge rates of the Ganges and Brahmaputra Rivers over a 17-year period (2000–2016). While there are no openly available river gauge records for the Meghna River, nor for the lower Ganges and Brahmaputra Rivers beyond 1992 (e.g., GRDC, 2009) analysis of discharge data obtained through orbital remote sensing was used to estimate average discharge rates (Dartmouth Flood Observatory; Brakenridge et al., 2012; Van Dijk et al., 2016). The lower Brahmaputra River (i.e., the Jamuna River in Bangladesh) experienced higher than normal overall discharge in 2012, which was the third highest year for monsoonal discharge (i.e., May–October) within the 17-year period we analyzed. However, overall Ganges River discharge (below the Farakka Barrage in India) was much lower than average in 2012, and was ranked 12th

in terms of mean monsoon season discharge between 2000–2016. It is possible that elevated Brahmaputra discharge in 2012 may have influenced sedimentation at trap sites. However, the combined Ganges and Brahmaputra discharge for 2012 was ~3% below the 17-year mean, and 2012 experienced only the 8th highest river discharge out of the 17 years that we analyzed, falling exactly in the middle of the 17-year spread of annually variable discharge rates. Additional fingerprinting in future studies using e.g., distinctive clay mineralogy would help determine discrete source river contributions to net sedimentation.

Sediment, subsidence, and sea level rise

More salient to the Bengal Delta's stability in the face of rising sea level, our results demonstrate mean vertical accretion in the fluvial-tidal delta plain is almost 5 times greater than the average rate of local sea level rise, estimated to be 0.5 cm yr^{-1} over ~24-years of tide gauge data obtained from two gauges located near to our study area: at the mouth of the main stem river (Charchanga station) and on the central Sundarbans delta front (Hiron Point station) (PSMSL). Sediment accumulation in this poldered area also offsets regional, yet locally heterogeneous, subsidence rates of up to 1.8 cm yr^{-1} (c.f., Higgins et al., 2014; Brown and Nicholls, 2015). If our sedimentation results are considered alongside relative sea level rise and subsidence rates independently, and 2012 is assumed to represent an average flood year, it appears that mean annual accumulation is more than sufficient for reducing the risk of coastal flooding in the central lower Bengal Delta. Combining subsidence rates and relative sea level rise presents a more complex and uncertain picture. Just as subsidence here is highly variable at both spatial and temporal scales (e.g., Brown and Nicholls (2015) present a comprehensive review of reported subsidence rates for the Bengal Delta), vertical sedimentation is likewise heterogeneous across the various land uses and

Rogers and Overeem: Doomed to drown? Sediment dynamics in the human-controlled floodplains of the active Bengal Delta

Art. 66, page 13 of 15

natural vs. engineered settings of our data set (**Table 1**). The threat of coastal flooding is therefore just as localized, and dependent upon interactions between vertical land surface movements, sediment accumulation, land use, and infrastructure. The relationship between these factors and vulnerability of the Bengal Delta to coastal flooding will be better understood through long-term, coordinated measurements of local-scale sedimentation and subsidence throughout the lower delta.

Conclusions
These initial field and model results can be used as a baseline for further experiments measuring local variations in lateral sedimentation and accretion, both within and outside of polders. Spatially variable sedimentation across the tidal and mixed fluvial-tidal regions of the Bengal Delta reflect the dominance of local physical processes, though polders are significant controls on sediment dispersal throughout. Secondary and tertiary natural channels, as well as engineered irrigation canals that penetrate the interior of poldered floodplains, are particularly effective in distributing sediment. Although mean annual sedimentation rates in the fluvial-tidal delta are more than five times that of local sea level rise, higher-resolution sedimentation–and subsidence–measurements across the delta plain would refine our ability to assess the Bengal Delta's vulnerability to climate change (e.g., Brammer, 2014; Brown and Nicholls, 2015). Overall, our results corroborate Wilson and Goodbred's (2015) findings that the fluvial-tidal region of the modern Bengal Delta is in a constructional stage. Wholly labeling the GBM as a "delta in peril" of drowning by sea level rise overlooks spatial variability in natural and engineered controls on sediment delivery to floodplains, as well as the robustness of the sedimentary system.

Data Accessibility Statement
The following data sets are available:

· Beryllium-7 results: as online supplementary information.
· AquaTellUs model code: available at https://github. com/csdms-contrib/aquatellus.

Supplemental Files
The supplemental files for this article can be found as follows:

· **Text S1.** Model theory. DOI: https://doi. org/10.1525/elementa.250.s1
· **Table S1.** Variables used in AquaTellUs. DOI: https:// doi.org/10.1525/elementa.250.s1
· **Table S2.** Experimental setup. DOI: https://doi. org/10.1525/elementa.250.s1
· **Table S3.** Beryllium-7 results and locations for recovered trap and surface samples. DOI: https://doi. org/10.1525/elementa.250.s1
· **Movie 1.** Rogers and Overeem_movie1. DOI: https:// doi.org/10.1525/elementa.250.s2
· **Movie 2.** Rogers and Overeem_Movie2. DOI: https:// doi.org/10.1525/elementa.250.s3

Author contributions
KR and IO contributed to every aspect of this manuscript.

References
Ahmed, A 2011 Some of the major environmental problems relating to land use changes in the coastal areas of Bangladesh: A review. *J Geog Region Plan* **4**(1): 1–8.
Allison, MA and **Kepple, EB** 2001 Modern sediment supply to the lower delta plain of the Ganges-Brahmaputra River. *Geo Mar Let* **21**: 66–74. DOI: https://doi.org/10.1007/s003670100069
Allison, MA, Khan, SR, Goodbred, SLG and **Kuehl, SA** 2003 Stratigraphic evolution of the late Holocene Ganges – Brahmaputra lower delta plain. *Sediment Geol* **155**: 317–342. DOI: https://doi.org/10.1016/S0037-0738(02)00185-9
Auerbach, L, Goodbred, SL, Mondal, D, Wilson, CA, Ahmed, KR, et al. 2015 In the Balance: Natural v. Embanked Landscapes in the Ganges-Brahmaputra Tidal Delta Plain. *Nature Clim Change* **5**: 153–157.
Bangladesh Bureau of Statistics (BBS) 2011 Census data [dataset]. Available at: bbs.gov.bd.
Bangladesh Water Development Board (BWDB) 2013 Coastal Embankment Improvement Project Phase I, Environmental and Social Management Framework Executive Summary. Dhaka, Bangladesh. Available at: http://bwdb.gov.bd/archive/pdf/364.pdf.
Barua, DK 1990 Suspended sediment movement in the estuary of the Ganges-Brahmaputra-Meghna river system. *Mar Geol* **91**(3): 243–253. DOI: https://doi.org/10.1016/0025-3227(90)90039-M
Barua, DK, Kuehl, SA, Miller, RL and **Moore, WS** 1994 Suspended sediment distribution and residual transport in the coastal ocean off the Ganges-Brahmaputra river mouth. *Mar Geol* **120**(1–2): 41–61. DOI: https://doi.org/10.1016/0025-3227(94)90076-0
Brakenridge, GR, Cohen, S, Kettner, AJ, De Groeve, T, Nghiem, SV, Syvitski, JP and **Fekete, BM** 2012

Calibration of satellite measurements of river discharge using a global hydrology model. *J Hydro* **475**: 123–136. DOI: https://doi.org/10.1016/j.jhydrol.2012.09.035

Brammer, H 2014 Bangladesh's dynamic coastal regions and sea-level rise. *Clim Risk Manage* **1**: 51–62. DOI: https://doi.org/10.1016/j.crm.2013.10.001

Brown, S and **Nicholls, RJ** 2015 Subsidence and human influences in mega deltas: the case of the Ganges–Brahmaputra–Meghna. *Sci Total Environ* **527**: 362–374. DOI: https://doi.org/10.1016/j.scitotenv.2015.04.124

CGIAR 2013 Adaptation and Mitigation Knowledge Network. Available at: https://ccafs.cgiar.org.

Coleman, JM 1969 Brahmaputra River: channel processes and sedimentation. *Sediment Geol* **3**: 129–139. DOI: https://doi.org/10.1016/0037-0738(69)90010-4

Dartmouth Flood Observatory Available at: http://floodobservatory.colorado.edu/DischargeAccess.html.

Global Runoff Data Centre (GRDC) 2009 Long-Term Mean Monthly Discharges and Annual Characteristics of GRDC Station/Global Runoff Data Centre, Koblenz, Federal Institute of Hydrology (BfG).

Goodbred, SL and **Kuehl SA** 1999 Holocene and modern sediment budgets for the Ganges-Brahmaputra river system: Evidence for highstand dispersal to flood-plain, shelf, and deep-sea depocenters. *Geology* **27**(6): 559–562. DOI: https://doi.org/10.1130/0091-7613(1999)027<0559:HAMSBF>2.3.CO;2

Goodbred, SL, Kuehl, SA, Steckler, MS and **Sarker, MH** 2003 Controls on facies distribution and stratigraphic preservation in the Ganges-Brahmaputra delta sequence. *Sediment Geol* **155**(34): 301–316. DOI: https://doi.org/10.1016/S0037-0738(02)00184-7

Hack, JT 1957 *Studies of longitudinal stream profiles in Virginia and Maryland* (294). US Government Printing Office.

Hale, RP, Goodbred, SL, Jr., Bain, RL, Wilson, C, Best, J and **Reed, MJ** 2015 River discharge controlling a tidal delta: the interplay between monsoon input and tidal reworking in SW Bangladesh. In: *AGU Fall Meeting Abstracts*.

Hanebuth, TJ, Kudrass, HR, Linstädter, J, Islam, B and **Zander, AM** 2013 Rapid coastal subsidence in the central Ganges-Brahmaputra Delta (Bangladesh) since the 17th century deduced from submerged salt-producing kilns. *Geology* **41**(9): 987–90. DOI: https://doi.org/10.1130/G34646.1

Higgins, SA, Overeem, I, Steckler, MS, Syvitski, JP, Seeber, L and **Akhter, SH** 2014 InSAR measurements of compaction and subsidence in the Ganges-Brahmaputra Delta, Bangladesh. *J Geophys Res-Ear Surf* **119**(8): 1768–1781. DOI: https://doi.org/10.1002/2014JF003117

Islam, MM, Chou, FN, Kabir, MR and **Liaw, CH** 2010 Rainwater: A potential alternative source for scarce safe drinking and arsenic contaminated water in Bangladesh. *Water Resour Manag* **24**(14):

3987–4008. DOI: https://doi.org/10.1007/s11269-010-9643-7

Islam, MR, Begum, SF, Yamaguchi, Y and **Ogawa, K** 1999 The Ganges and Brahmaputra rivers in Bangladesh: basin denudation and sedimentation. *Hydrol Process* **13**: 2907–2923. DOI: https://doi.org/10.1002/(SICI)1099-1085(19991215)13:17<2907::AID-HYP906>3.0.CO;2-E

Khan, SR and **Islam, MB** 2008 Holocene stratigraphy of the lower Ganges-Brahmaputra river delta in Bangladesh. *Front Earth Sci China* **2**(4): 393–399. DOI: https://doi.org/10.1007/s11707-008-0051-8

Kim, W, Mohrig, D, Twilley, R, Paola, C and **Parker, G** 2009 Is it feasible to build new land in the Mississippi River Delta. *Eos* **90**(42): 373–374. DOI: https://doi.org/10.1029/2009EO420001

Kuehl, SA, Allison, MA, Goodbred, SL and **Kudrass, HE** 2005 The Ganges-Brahmaputra Delta. *Special Publication-SEPM* **83**: 413.

Mondal, MK, Tuong, TP and **Sattar, MA** 2008 Quality and groundwater level dynamics at two coastal sites of Bangladesh: implications for irrigation development. *CGIAR Challenge Program on Water and Food.* Available at: https://cgspace.cgiar.org/bitstream/handle/10568/56165/IFWF2_proceedings_Volume%20II.pdf.

Murty, TS and **Henry, RF** 1983 Tides in the Bay of Bengal. *J Geophys Res* **88**(C10): 6069–6076. DOI: https://doi.org/10.1029/JC088iC10p06069

Overeem, I and **Syvitski, JPM** 2009 Dynamics and Vulnerability of Delta Systems. *LOICZ Reports and Studies* **35**: 54. Geesthacht Germany.

Overeem, I, Syvitski, JPM and **Hutton, E** 2005 Three-dimensional Numerical Modeling of Deltas. *SEPM Spec Publ* **83**: 13–30.

Overeem, I, Veldkamp, A, Tebbens, L and **Kroonenberg, SB** 2003 Modelling Holocene stratigraphy and depocentre migration of the Volga delta due to Caspian Sea-level change. *Sediment Geol* **159**(3–4): 159–175. DOI: https://doi.org/10.1016/S0037-0738(02)00257-9

Passalacqua, P, Lanzoni, S, Paola, C and **Rinaldo, A** 2013 Geomorphic signatures of deltaic processes and vegetation: The Ganges-Brahmaputra-Jamuna case study. *J Geophys Res-Ear Surf* **118**(3): 1838–1849. DOI: https://doi.org/10.1002/jgrf.20128

Permanent Service for Mean Seal Level (PSMSL) Tide gauge data [dataset]. Available at: http://www.psmsl.org accessed February 2013.

Poulton, PL, Rawson, HM, Dalgliesh, NP, Carberry, PS, Dove, H, et al. 2010 Integrating wheat into the rice-based farming systems of southern Bangladesh. In: *Proc of the Australian Society of Agronomy Conference*, 15–19. Lincoln, New Zealand.

Rahman, A 1994 Beel Dakatia: The Environmental Consequences of a Development Disaster. University Press.

Rogers, KG, Goodbred, SL and **Mondal, DR** 2013 Monsoon sedimentation on the 'abandoned' tide-influenced Ganges–Brahmaputra delta plain. *Estuar*

Rogers and Overeem: Doomed to drown? Sediment dynamics in the human-controlled floodplains of the active Bengal Delta

Art. 66, page 15 of 15

Coast Shelf S **131**: 297–309. DOI: https://doi.org/10.1016/j.ecss.2013.07.014

Schuller, P, Iroumé, A, Walling, DE, Mancilla, HB, Castillo, A, et al. 2006 Use of beryllium-7 to document soil redistribution following forest harvest operations. *J Environ Qual* **35**(5): 1756–63. DOI: https://doi.org/10.2134/jeq2005.0410

Sommerfield, CK, Nittrouer, CA and **Alexander, CR** 1999 ⁷Be as a tracer of flood sedimentation on the northern California continental margin. *Cont Shelf Res* **19**(3): 335–61. DOI: https://doi.org/10.1016/S0278-4343(98)00090-9

Syvitski, JPM, Kettner, AJ, Overeem, I, Hutton, EWH, Hannon, MT, et al. 2009 Sinking deltas due to human activities. *Nat Geosci* **2**: 681–686. DOI: https://doi.org/10.1038/ngeo629

Tessler, ZD, Vörösmarty, CJ, Grossberg, M, Gladkova, I, Aizenman, H, et al. 2015 Profiling risk and sustainability in coastal deltas of the world. *Science* **349**(6248): 638–643. DOI: https://doi.org/10.1126/science.aab3574

Van Dijk, AI, Brakenridge, GR, Kettner, AJ, Beck, HE, De Groeve, T and **Schellekens, J** 2016 River gauging at global scale using optical and passive microwave remote sensing. *Wat Reso Res* **52**(8): 6404–6418. DOI: https://doi.org/10.1002/2015WR018545

Walling, DE 2013 Beryllium-7: The Cinderella of fallout radionuclide sediment tracers? *Hydro Proc* **27**(6): 830–844. DOI: https://doi.org/10.1002/hyp.9546

Wilson, CA and **Goodbred, SL** 2015 Construction and Maintenance of the Ganges-Brahmaputra-Meghna Delta: Linking Process, Morphology, and Stratigraphy. *Annu Rev Mar Sci* **7**: 67–88. DOI: https://doi.org/10.1146/annurev-marine-010213-135032

Woodroffe, CD, Nicholls, RJ, Saito, Y, Chen, Z and **Goodbred, SL** 2006 Landscape variability and the response of Asian megadeltas to environmental change, In: Harvey, N (ed.), *Global change and integrated coastal management: the Asia-Pacific region, coastal systems and continental margins.* Dordrecht: Springer. DOI: https://doi.org/10.1007/1-4020-3628-0_10